PCCP

PAPER

View Article Online
View Journal | View Issue

Cite this: *Phys. Chem. Chem. Phys.*, 2017, **19**, 15454

Collision-induced dissociation of sodiated glucose and identification of anomeric configuration†

Jien-Lian Chen, [a] Hock Seng Nguan, [a] Po-Jen Hsu, [a] Shang-Ting Tsai, [a] Chia Yen Liew, [a] Jer-Lai Kuo, [a] Wei-Ping Hu [b] and Chi-Kung Ni *[ac]

Received 13th April 2017,
Accepted 26th May 2017

DOI: 10.1039/c7cp02393f

rsc.li/pccp

Collision-induced dissociation (CID) of sodiated glucose was investigated using electronic structure calculations and resonance excitation in a low-pressure linear ion trap. The major dissociation channels in addition to desodiation are dehydration and $C_2H_4O_2$ elimination reactions which the barrier heights are near to or lower than the sodiation energy of glucose. Dehydration reaction involves the transfer of the H atom from the O2 atom to the O1 atom, followed by the cleavage of the C1–O1 bond. Notably, α-glucose has a dehydration barrier lower than that of β-glucose. This difference results in the larger branching ratio of dehydration reactions involving α-glucose, which provides a simple and fast method for identifying the anomeric configurations of glucose. The $C_2H_4O_2$ elimination starts from the H atom transfer from the O1 atom to the O0 atom, followed by the cleavage of the C1–O0 bond. These results were further confirmed by experimental study using ^{18}O-isotope-labeled compounds. Both the experimental data and theoretical calculations suggest that the dehydration reaction and cross-ring dissociation of sodiated carbohydrates mainly occur at the reducing end during low-energy CID.

I. Introduction

The four basic categories of molecules involved in creating life are nucleic acids, proteins, carbohydrates, and lipids. To understand their chemical and biological properties of these molecules, it is necessary to obtain their complete structural information. Methods for sequencing and determining the structure of nucleic acids and proteins have been well developed; however, owing to the complex structure of carbohydrates, the development of robust analytical methods to obtain the structure of these molecules remains a challenge.[1] The complete structural determination of carbohydrates requires the identification of each monosaccharide, as well as knowledge of the linkage types, anomeric configurations, sequence, and branch locations. The number of possible carbohydrate structures for a given chemical formula is substantial, such that structural determination has become a major obstacle in carbohydrate research.[2]

The structures of carbohydrates can be determined using nuclear magnetic resonance spectroscopy,[3] infrared spectroscopy,[4,5] chromatography,[6] and mass spectrometry.[7] Mass spectrometry (MS) is widely applied in the structural analysis of carbohydrates because of its high sensitivity. It requires only a small amount of sample compared with other methods. Collision-induced dissociation (CID) is one of the major analytical techniques in the structural determination of carbohydrates using tandem mass spectrometry.[7] In the process of low-energy CID in an ion trap, parent ions in the trap are accelerated by an electric field. They accumulate internal energy from collisions with neutral gases, which typically include He and Ar. In each collision, a small amount of translational energy is transferred to the vibrational energy of the trapped ions.[8–10] Many collisions are required before a trapped ion obtains enough energy to undergo dissociation. Because the energy transfer in low-energy CID occurs from translation to vibration and the electronically excited states are not involved in the energy transfer, dissociation always occurs in the electronic ground state. Moreover, if the accumulation of vibrational energy is slow compared to dissociation, dissociation only takes place from those channels with low barriers.

The fragments produced from CID are analyzed to determine carbohydrate structures. Several empirical fragmentation patterns have been identified and are used in the determination of carbohydrate structures. For example, in the dissociation of lithiated or sodiated disaccharides, the elimination of fragments m = 120 u; m = 18 u and 90 u; m = 18, 60 u; and m = 18, 60, 90, and 120 u represent structures with 1–2 linkage, 1–3 linkage, 1–4 linkage, and 1–6 linkage, respectively.[11–14] Different empirical fragment patterns have also been found for the anions of deprotonated carbohydrates[15–17] and for permethylated carbohydrates.[18]

[a] *Institute of Atomic and Molecular Sciences, Academia Sinica, P. O. Box 23-166, Taipei 10617, Taiwan. E-mail: ckni@po.iams.sinica.edu.tw*
[b] *Department of Chemistry and Biochemistry, National Chung Cheng University, Chia-Yi 621, Taiwan*
[c] *Department of Chemistry, National Tsing Hua University, Hsinchu 30013, Taiwan*

† Electronic supplementary information (ESI) available. See DOI: 10.1039/c7cp02393f

Leary and co-workers studied the CID of lithiated gentiobiose using ^{18}O-labeled compounds and semi-empirical calculations.[11] Their experimental data showed that the dehydration reaction mainly occurs as a result of the cleavage at the reducing end, whereas cross-ring dissociation only occurs at the reducing end. Quadrupole ion trap mass spectrometry was used to study the dissociation pathways of ^{18}O-labeled cellobiose by Asam *et al.*,[12] who demonstrated that cross-ring dissociation only occurred at the reducing end for both Li and Na cationized species. A study of lithiated α-(1,5)-L-arabinobiose and β-(1,4)-D-xylobiose by da Costa *et al.*[9] demonstrated that the dehydration reaction and cross-ring dissociation mainly occur at the reducing end; however, they also observed a small fraction of dissociation at the nonreducing end. In addition, Scaraffia and co-workers examined ^{13}C-labeled glucose at C1 and C2 using tandem mass spectrometry[19] and revealed that the $C_2H_4O_2$ elimination in cross-ring dissociation involves both the C1 and C2 atoms. By contrast, Lee *et al.* assigned the fragments of cross-ring dissociation from the CID of various sodiated disaccharides to the dissociation at both the nonreducing and reducing sides.[20]

Most of the previous theoretical studies about carbohydrates have been focused on determining the structures of conformation and the interaction energies with other hydrocarbons[21–28] and metal ions.[29–31] High-level quantum chemical calculations have been used to investigate the decomposition of glucose,[32] protonated xylose,[33] protonated fructose,[34] and protonated glucose.[35] Most of these studies have concentrated on the applications of carbohydrates in renewable energy.[32–34] Theoretical investigation of carbohydrate decomposition in mass spectrometry is scarce.[35–37]

In this study, we used sodiated glucose as a model molecule to examine the low-energy CID of sodiated underivatized carbohydrates. High-level quantum chemical calculations were used to identify the dissociation barrier heights of various dissociation channels. The dissociation products predicted by the theoretical calculations were then compared to the CID mass spectra derived from the resonance excitation of sodiated glucose in a low-pressure linear ion trap. According to the calculations and the confirmation through experimental measurements, a simple method is proposed for identifying the anomeric configuration of glucose.

II. Experimental method

α- and β-glucose were purchased from Acros Organics (Geel, Belgium) and Fluorochem (Derbyshire, UK), respectively. They were used without purification. α- or β-glucose were added to methanol (containing NaCl 2×10^{-4} M) to produce 10^{-4} M glucose solution, and immediately followed by the mass spectrum measurement. The electrospray mass spectra were recorded using a LTQ XL Linear Ion Trap Mass Spectrometer (Thermo Fisher Scientific Inc.) equipped with an electrospray ionization source. The mass spectrometer was driven using the built-in procedure in the Tune Plus software (27.0.1103 SP1). Sample solutions were introduced into the ion source at a flow rate of 5 μL min^{-1}. The other instrument conditions were as follows: capillary T = 200 °C, ion spray voltage = 4 kV, capillary voltage = 136 V, tube lens voltage = 249 V, sheath gas, aux gas, and sweep gas were not used. Ions were scanned at a speed of 16 700 s^{-1}; 1 minute of scan was accumulated for each spectrum. For MS^2 experiments, the precursor ion isolation width was set to 1 u, and the normalized collision energy (NCE) varied between 20% and 100%, Q value was set at 0.25, and helium gas was used as buffer gas for ion trap as well as collision gas in CID. The pressure of helium was 9.3×10^{-6} Torr, measured by an ion gauge located inside the vacuum chamber, but outside the ion trap.

The method used to prepare the ^{18}O-labeled glucose at the reducing end (*i.e.*, oxygen atom connected to anomeric carbon) is similar to the method that has been described in previous studies.[38,39] In brief, glucose was added to 60 μL of $^{18}OH_2$ (MSD, 97%) to produce 0.1 M glucose solution. This solution was kept in a sealed vial. The sealed vial was sat in a vacuum desiccator with silica gel for more than 3 weeks. Subsequently, 3 μL solution was added to 297 μL of CH_3OH (containing of NaCl 2×10^{-3} M) to obtain 10^{-4} M ^{18}O-labeled glucose in CH_3OH and the solution was used within a few minutes.

III. Calculation method

Geometries and relative energies of reactants, transition states, and dissociation products in the gas phase were calculated using density functional theory. First, the molecular geometry, reaction barrier, and harmonic vibrational frequencies of the stationary points were calculated using B3LYP functional[40] with the 6-311+G(d,p) basis set. This method is computationally efficient. It has been shown that the calculated energies of glucose and maltose are accurate to within 20 kJ mol^{-1}.[41] Next, the relative energies of selected stationary points were refined using the single-point calculation at the MCG3-MPWB[42] level which is a very accurate and efficient multi-coefficient method that combines the wavefunction-based and electron density-based electronic structure calculations. All the electronic structure calculations in the current study were performed using the Gaussian 09 program.[43]

IV. Results and discussion

The ring structures of glucose can pucker into different forms. The numbers of stable conformers for α-D-glucose and β-D-glucose was found to be 201 and 202, respectively.[44,45] They can be categorized into 28 classes: 2 chair conformations, 6 boat conformations, and 6 skew conformations for both α-and β-glucoses, as shown in Fig. 1. In each class of conformation, the orientation changes of various OH groups and CH_2OH group result in different conformers.

In sodiated glucose, the sodium cation prefers to attach to oxygen atoms due to the strong interaction between them. Since there are six oxygen atoms in glucose, it indicates that there are at least 6 locations for sodium cations to form stable conformers.

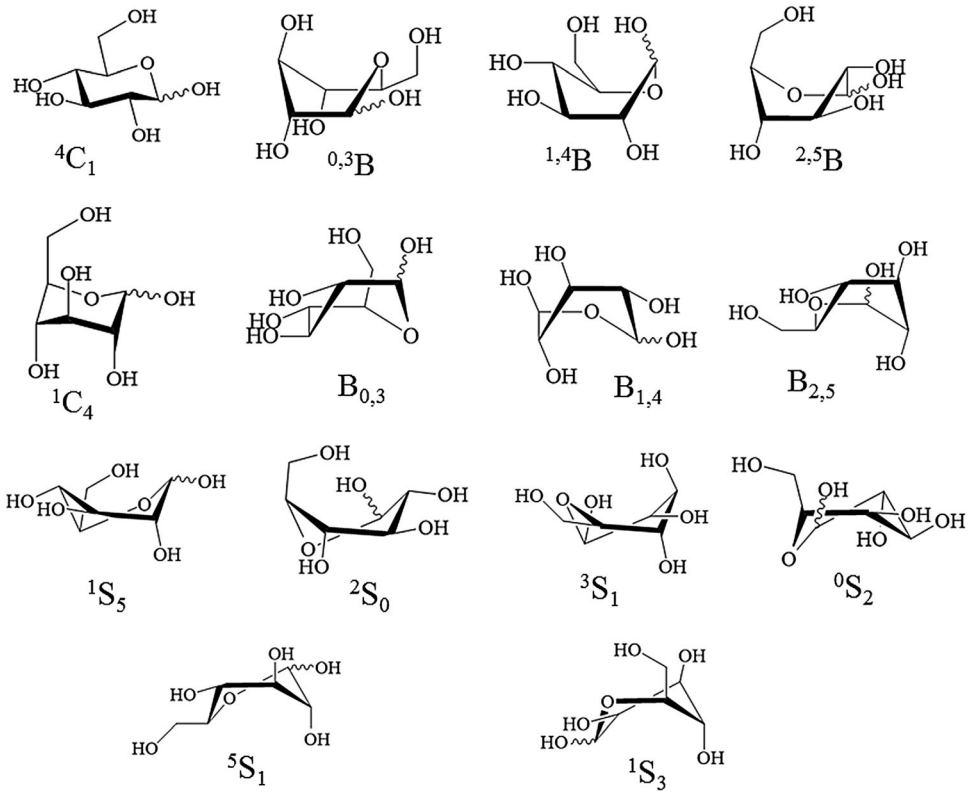

Fig. 1 The major conformations of glucose, including 2 chair conformations, 6 boat conformations, and 6 skew conformations for both α- and β-glucoses.

In the dissociation process of dehydration reaction, an H atom has to be transferred to an OH group. There are 5 OH groups and therefore 10 possible channels for each OH group: the transferred H atom can be from one of the 6 C atoms or from one of another four OH groups. For cross-ring elimination of $C_2H_4O_2$, there are 5 possible combinations of the neighboring two C atoms. The total number of transition states for dehydration reaction and cross-ring dissociation from these conformers is estimated to be more than two thousands, which is too large to be calculated with high accuracy in a reasonable time.

To obtain accurate calculations in a reasonable period of time, following strategies and findings were used. First, we found that sodiated skew conformations are not stable, although the free skew conformations (*i.e.*, without sodiation) are stable. Sodiated skew conformations convert to sodiated boat conformations upon geometry relaxation. Consequently, no further calculations of sodiated skew conformations are needed.

Second, when sodium cation is attached to glucose, the orientations of the OH groups near sodium cation are fixed due to the strong interaction between sodium cation and O atoms. However, the OH (or CH_2OH) group which is far away from the sodium cation still can rotate and result in different stable conformers. We chose an arbitrary orientation of this far-away OH group for two chair conformations and two boat conformations ($^4C_1$ and $^{0,3}B$ for both α and β configuration), then we calculated the transition states of these four conformers under the full consideration of all possible sodium cation locations and H atom transfer pathways (H is transferred from C atoms or OH groups) using B3LYP functional with the 6-311+G(d,p) basis set. The calculated results from these four conformations enable us to learn how H atom is transferred, and to find the location of the sodium ion in the transition states associated with the lower energy barriers. We found the barrier of H atom transfer from any of the C atoms to be too high for such processes to make any significant contribution to the observed dehydration reaction. Only the H atom of OH groups can be transferred, and sodium cation has to be near the O atom of the OH group from which the H atom is transferred. The is consistent with the experimental results using D labeled carbohydrates.[11,14,37] Details of these transition states are shown below. Consequently, the calculations for the rest of 12 chair and boat conformations were carried out only for the H atom transferring from OH group and the locations of sodium cation near the O atom of the OH group from which the H atom is transferred.

Third, energies of the most important transition states (*i.e.*, low barrier height) were refined at the MCG3-MPWB[42] level, which is time consuming but is more accurate in energy. Finally, we investigated the effect of OH (or CH_2OH) orientation on the dissociation barrier heights using MCG3-MPWB level calculations only for these important transition states.

In each dissociation channel, there may be more than one transition states along the reaction coordinate. For simplicity, only the largest transition state energy was plotted in figures

and we assumed that the reactants passing the highest transition state can generate products.

A. Sodiation energy and migration of sodium cation

(1) α-Glucose. The isomerization barriers from sodiated α-glucose with chair conformation to sodiated α-glucose with boat conformation are not high (47.6 and 61.9 kJ mol^{-1}), as illustrated in Fig. 2. The low barrier heights of isomerization between chair and boat conformations indicate that α-glucose can easily change from one conformation to the other. The charge of each atom in glucose and in sodiated glucose is shown in ESI.† When sodium cation attaches to glucose, the charge of each atom in glucose does not change very much. It suggests that sodium cation is solvated by the glucose. No protonated salt, $[C_6H_{11}O_6Na]H^+$, is formed.

The sodiation energies, defined as the heat of reaction of [glucose]Na^+ → glucose + Na^+, range from 185.6 to 203.1 kJ mol^{-1} for α-glucose in chair conformations. It depends on the position of the attached sodium cation. The geometries and relative energies of sodiated α-glucose in chair conformation, $^4C_1$, are illustrated in Fig. 3. Similar sodiation energies of glucose have been reported previously.[29,30] In general, the barrier heights of sodium cation migration are less than 120 kJ mol^{-1}.

The geometries and relative energies of sodiated α-glucose in boat conformation, $^{0,3}B$, are illustrated in Fig. 4. The sodiation energies range from 159.2 to 189.8 kJ mol^{-1}, depending on the position of the attached sodium ion. Notably, the barrier heights of sodium cation migration are also small in boat conformation. This suggests that the sodium cation can move easily in sodiated α-glucose in both chair and boat conformations.

(2) β-Glucose. The sodiation energies and sodium cation migration barriers of β-glucose molecules were found to be similar to those of α-glucose, as illustrated in Fig. S1–S3 of the ESI.†

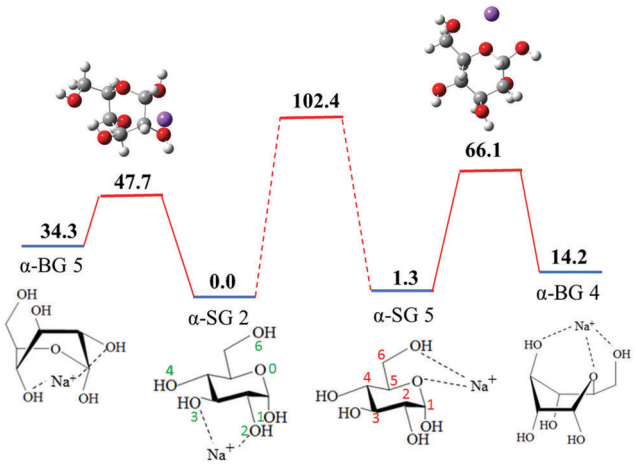

Fig. 2 Calculated barriers (in kJ mol^{-1}) for the isomerization from sodiated α-glucose with a chair conformation (α-SG2 and α-SG5) to sodiated α-glucose with a boat conformation (α-BG4 and α-BG5). The barriers for the change between two chair conformations (α-SG2 and α-SG5) illustrated in dot line were shown in details in Fig. 3. The zero of potential energy is set at the most stable conformer of sodiated α-glucose (*i.e.*, α-SG2; see Fig. 3). Calculated at the B3LYP/6-311+G(d,p) level. The numberings for carbon and oxygen atoms are shown in red and green, respectively.

B. Dehydration reaction

Dehydration reaction is one of the major reactions that occur in the CID of carbohydrates. Since the glucose molecule contains several OH groups, a dehydration reaction can occur by (1) an H atom from one OH group being transferred to another OH group, or (2) an H atom connected to a carbon atom being

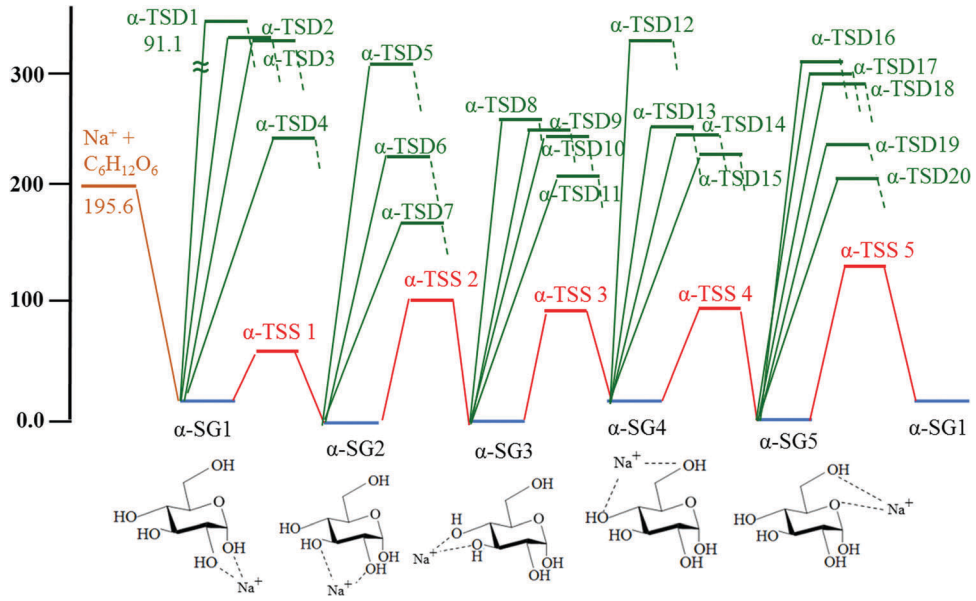

Fig. 3 Relative energies (in kJ mol^{-1}) of sodiated α-glucose with chair conformation $^4C_1$ (blue lines), sodium cation migration barriers (red lines), sodiation energy (brown line), and dehydration reaction barriers (green lines). The energy levels of the dehydration products are not shown. Calculated at the B3LYP/6-311+G(d,p) level. The zero of potential energy is set at the most stable conformer (*i.e.*, α-SG2).

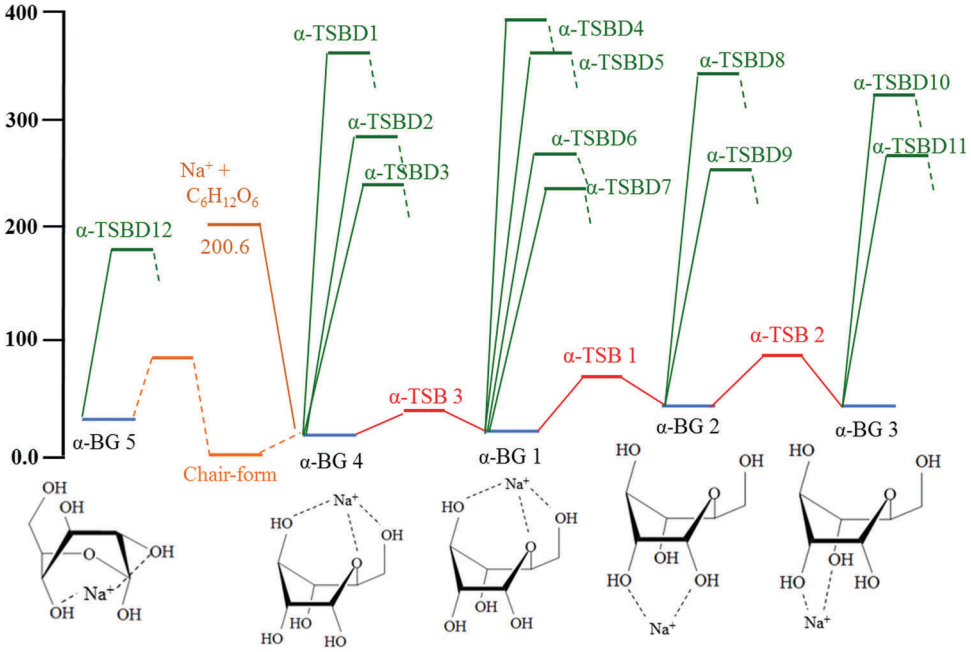

Fig. 4 Relative energies (in kJ mol^{-1}) of sodiated α-glucose with boat conformation ^{0,3}B (blue lines), sodium cation migration barriers (red lines), sodiation energy (brown line), and dehydration reaction barriers (green lines). The energy levels of the dehydration products are not shown. The orange line signifies that the isomerization between α-BG4 and α-BG5 has to pass through a chair conformation. Calculated at the B3LYP/6-311+G(d,p) level. The zero of potential energy is set at the most stable conformer (α-SG2). The dissociation channel with low barrier height from another boat conformation $B_{1,4}$, α-BG5, is also illustrated.

transferred to an OH group, followed by the cleavage of the C–OH_2 bond. In the present study, we investigated both possibilities for $^4C_1$ chair conformation and ^{0,3}B boat conformation to determine the dehydration mechanisms. Calculations were performed for the H atom transfer from C atoms or OH groups with the sodium ion located in various positions. We found that the H atom transfer corresponding to the H atom transfer from C atoms has significantly larger barrier heights (>280 kJ mol^{-1}). These channels will not be further discussed in this study. In contrast, some of the dehydration channels corresponding to the H atom from OH groups have relatively low barrier heights, as illustrated in Fig. 3 and 4 (for α-glucose $^4C_1$ and ^{0,3}B) and in Fig. S2 and S3 of the ESI† for β-glucose $^4C_1$ and ^{0,3}B. Detailed geometries of these transition states are presented in Fig. S4 and S5 of the ESI.†

We found that the geometries of the transition states of the low-barrier dehydration reactions have two properties. First, the distance between the two OH groups is close (<2.5 Å) and the sodium cation is near the O atom of the OH group from which the H atom is transferred. The calculations for the search of transition states with low barrier heights for the rest of conformations ($^1C_4$, $B_{0,3}$, ^{1,4}B, $B_{1,4}$, ^{2,5}B, and $B_{2,5}$) were carried out only for the geometries which satisfy these two properties. The barrier heights of the transition states for the other conformations were found to be high (Fig. S6 and S7, ESI†), except one transition state of $B_{1,4}$ conformation of α-glucose. This conformation (α-BG5) and the transition state (α-TSBD12) for dehydration are shown in Fig. 4.

Among the various dehydration reactions, we found that the transfer of an H atom from O2 to O1 of α-glucose in chair conformation, $^4C_1$, has the lowest barrier height (168.9 kJ mol^{-1}), as indicated by the α-TSD7 in Fig. 3. This reaction is the major pathway for dehydration reaction. The dissociation mechanism involves the concerted reactions of the H atom transfer from O2 to O1, the C1–O1 bond cleavage, and the H atom transfer from C2 to C1, as illustrated in Fig. 5(a). The H atom transfer from O4 to O1 in boat conformation, $B_{1,4}$, has the second lowest barrier height (180.6 kJ mol^{-1}), as illustrated by the α-TSBD12 in Fig. 4. Notably, these two channels are the only dehydration reactions for which the barrier heights are considerably lower than the sodiation energy (203.1 kJ mol^{-1}). The barrier heights of other dehydration reactions are either close to the sodiation energy (α-TSD11, 208.6; α-TSD20, 206.9 kJ mol^{-1}) or substantially higher than the sodiation energy. The transition states, α-TSD11, and α-TSD20 correspond to the H atom transfer from O3 to O2, and O1 to O2, respectively.

The four dehydration channels with the lowest barrier heights for β-glucose correspond to β-TSD7 (195.2 kJ mol^{-1}) and β-TSD21 (203.1 kJ mol^{-1}) in the chair conformation (Fig. S2, ESI†) and β-TSBD3 (186.8 kJ mol^{-1}) and β-TSBD7 (180.6 kJ mol^{-1}) in the boat conformation (Fig. S3, ESI†). These barrier heights are close to the sodiation energy (204.0 kJ mol^{-1}) of β-glucose. The reaction path of β-TSD7 involves the H-atom transfer from O2 to O1, the reaction path of β-TSD21 involves the H-atom transfer from O1 to O2, and the reaction paths of both β-TSBD3 and β-TSBD7 involve the H-atom transfer from O3 to O1.

Among these low-barrier dissociation channels, transition states α-TSD7 and β-TSD7 have similar structures. Both of the sodium cations are located between O2 and O3, and the

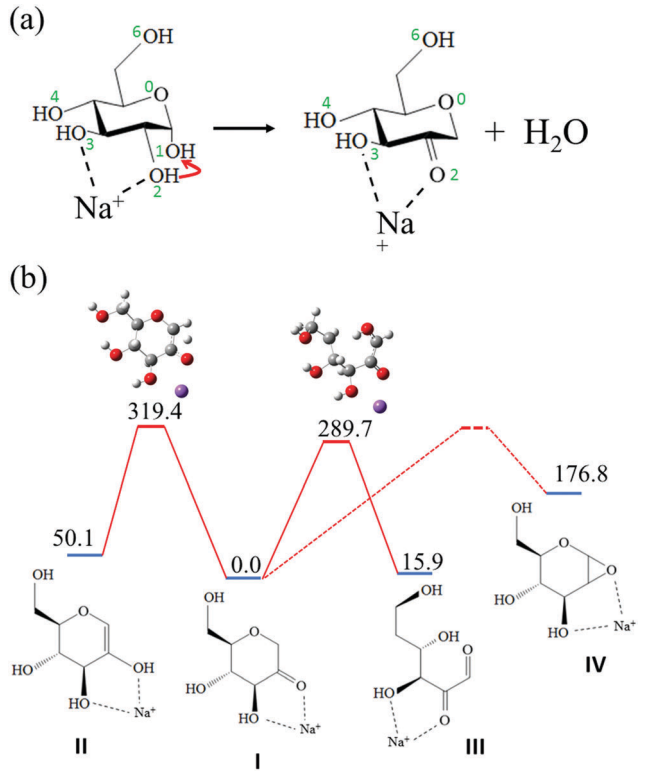

Fig. 5 (a) The major dehydration reaction. The numberings for oxygen atoms are shown in green. (b) Structures and relative energies (in kJ mol^{-1}) calculated at B3LYP/6-311+G(d,p) level of various dehydration products and the isomerization transition states between them. The energy of transition state between product (I) and (IV) was not calculated, however, the large heat of reaction suggests the barrier height is at least 176.8 kJ mol^{-1}.

reactions involve the transfer of an H atom from O2 to O1 in the chair conformation. However, the dehydration reaction barrier height of α-glucose is smaller than that of β-glucose by 26.3 kJ mol^{-1}. This is because the relative geometries of the two OH functional groups involved in the dehydration reaction are different. Specifically, the OH functional groups attached to C1 and C2 are in *cis*-configuration in α-glucose, but they are in trans-configuration in β-glucose. The distance traveled by the H atom is shorter in α-glucose (~2.13 Å) than that in β-glucose (~2.35 Å). The reaction corresponding to the transition state α-TSD7 is predicted to be the major dehydration pathway for sodiated α-glucose. Notably, the dehydration product (Product I in Fig. 5(b)) from this major reaction pathway is very different from those predicted in previous studies.[46,47] The formation of other products would require either higher barrier or significantly higher energies of reactions, as illustrated in Fig. 5(b).

We also calculated H atom transfer within the linear conformer of glucose formed when the C–O#0 bond breaks (*vide infra*). The calculated energy barriers for H atom transfer from one OH to another OH in this case are all sufficiently high (see Fig. S8 of the ESI†) that such transfers are deduced not to occur.

C. Cross-ring dissociation

Cross-ring dissociation breaks the ring of glucose into two parts. The typical cross-ring dissociation channels of oligosaccharides include the elimination of $C_2H_4O_2$, $C_3H_6O_3$, and $C_4H_8O_4$ fragments. The cross-ring dissociation produces important fragments for the determination of linkage types between connecting monosaccharides.[11–14]

There are four C–C bonds and two C–O bonds in a glucose ring; cross-ring dissociation requires the cleavage of at least two of these bonds (either two of the C–C bonds, or one C–C bond and one C–O bond). In the calculation process, we began with the cleavage of one (C–O or C–C) bond, followed by the cleavage of a second bond. For the first cleavage, the calculation was carried out with the sodium cations located at various positions. In total, 124 transition states were calculated for $^4C_1$ and $^{0,3}B$ conformers of both α and β configurations. The energies of these transition states are listed in Table S1 of the ESI.†

Of these transition states, the lowest dissociation barriers for α- and β-glucose (167–210 kJ mol^{-1}) were found to be the C1–O0 bond cleavage. The reaction begins from the concerted O1 to O0 H atom transfer and C1–O0 bond cleavage, as illustrated in the first step of Fig. 6. We found that the barrier heights for other C–C or C–O bond cleavage as the first step in cross-ring dissociation are in the range from 320 to 410 kJ mol^{-1}. Since they are significantly larger, we do not consider these pathways further in the current study.

Once the C1–O0 bond breaks, the skeleton of glucose forms a linear structure. The linear structure can be altered to various conformations by rotating various C–C bonds. The barriers for the interconversions between these conformations are usually small. When the molecule is in a structure with O1 being close to the H atom of O3, as illustrated after the second step of Fig. 6, the migration of H atom from O3 to O1 and the cleavage of C2–C3 bond can occur and result in $C_2H_4O_2$ elimination, as shown in the third step of Fig. 6. The barrier of the third step is

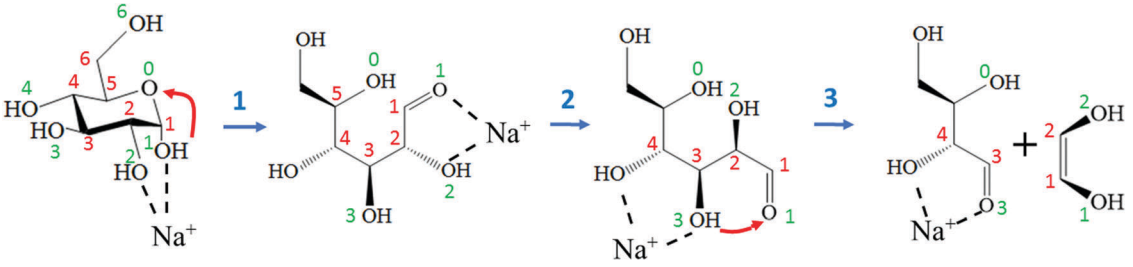

Fig. 6 Major reaction mechanism of cross-ring dissociation. The numberings for oxygen atoms and carbons atoms are shown in green and red, respectively.

only 127.5 kJ l mol^{-1}. This reaction mechanism is similar to that proposed in previous studies of disaccharides.[11,37]

D. Refined energies of major dissociation channels

In low-energy CID, reactions primarily occur on the dissociation channels that have low barrier heights. Desodiation is one of the dissociation channels with low barrier height. Other dissociation can only occur if the reaction barrier heights are close to or lower than the desodiation energy, otherwise the desodiation would be the dominate dissociation channel. We refined the calculated barrier heights of those dissociation channels with low barrier heights found at B3LYP/6-311+G(d,p) level using the more accurate MCG3-MPWB method. The transition states with low barrier heights are correlated to the conformers α-SG1, α-SG2, β-SG1, β-SG2, β-BG4, and β-BG1, as shown in Fig. 7. The effects of the OH (or CH_2OH) orientation on the barrier heights were investigated for these conformers. We found different orientations of CH_2OH also result in stable conformers, α-SG1′, α-SG2′, β-SG1′, and β-SG2′, as shown in Fig. 7. However, the changes of barrier height due to the orientation of CH_2OH are small. Detailed structures of these transition states are shown in Fig. S9 (ESI†). The charge of each atom in neutral glucose, reactants and transition states of sodiated glucose are found to be similar, as illustrated in Fig. S9 of ESI,† indicating that the "object" which is transferred during the dissociation process is H atom, not proton.

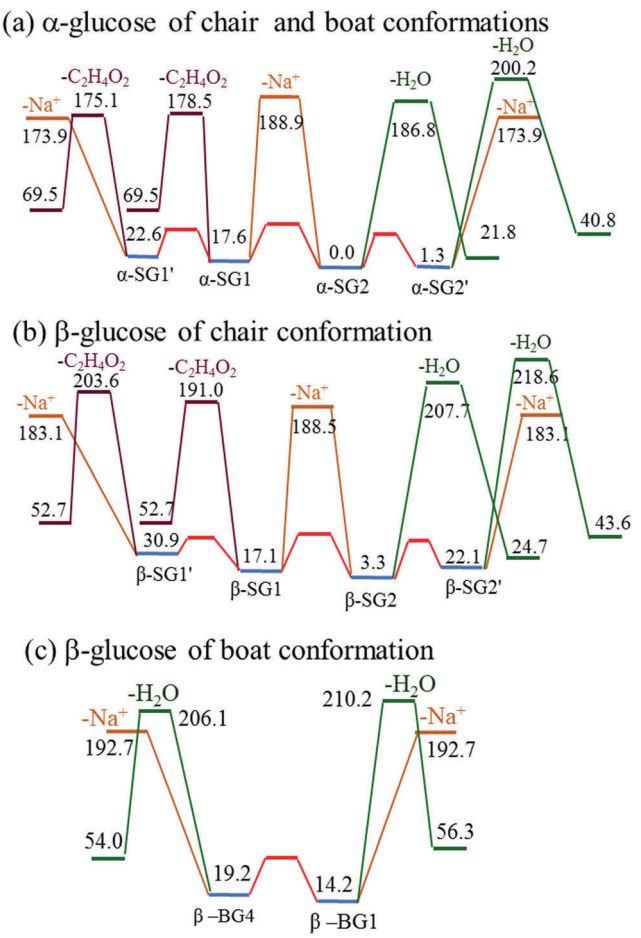

Fig. 7 The refined energies (kJ mol^{-1}) of the dissociation channels with low barrier heights for desodiation, dehydration reaction, and cross-ring dissociation using more accurate multilevel method MCG3-MPWB and the effects of CH_2OH orientation on energies.

Fig. 7 reveals that both the barriers of cross-ring dissociation and the dehydration reaction for α-SG1 and α-SG2 are lower than the corresponding desodiation energy for α-glucose. Thus, both reactions can occur before the elimination of the sodium cation. In contrast, the barrier heights of both dehydration and cross-ring dissociation are higher than the desodiation energy for all conformers of β-glucose. Consequently, desodiation should be one of the major dissociation channels for β-glucose. Since the lowest barrier height of cross-ring dissociation is only 2.5 kJ mol^{-1} higher than the desodiation energy for β-glucose, it could certainly compete with the desodiation channel. However, the lowest dehydration barriers are 12–20 kJ mol^{-1} larger than the desodiation energy, dehydration should not be the major dissociation channel for β-glucose. Our calculations thus suggest that α-glucose would show a larger branching ratio associated with dehydration than β-glucose does.

E. CID spectra

The mutarotation of glucose is slow[48] compared to the time between preparing the glucose solution and making the mass spectroscopic measurement, so most of the solid α-glucose (or β-glucose) dissolved in solution remained as α-glucose (or β-glucose) when we measured the mass spectra within first few minutes after dissolution. Fig. 8(a) and (b) show the CID spectra of sodiated α-glucose and β-glucose, respectively, obtained at 40% NCE. Two main dissociation channels were observed. They represent H_2O elimination (m/z 185) and $C_2H_4O_2$ elimination (m/z 143 and 83). The loss of sodium ions was not observed because of the low-mass cutoff of the ion trap. We found that the desodiation is one of the major dissociation channels from the following observation. We fixed the ion injection time of ion trap and measured the parent ion intensity at 0% and 30% NCE, respectively. The spectrum at 0% only contains parent ions. The spectrum at 30% NCE includes the residual parent ions and those fragment ions with m/z values above the low-mass cut-off. One major ionic fragment with an m/z below this cut-off is the Na^+ ion. We found the total fragment ion intensity in the spectrum of 30% NCE is at least 10 times smaller than the decrease of parent ion intensity in the spectra from 0% NCE to 30% NCE. The large difference between the appearance of fragment ions and loss of parent ions indicates that desodiation is one of the major dissociation channels. However, the accurate branching ratio of desodiation cannot be estimated because the mass dependence of trapping and ejection efficiencies of ion trap and detection efficiency of ion detector were not calibrated.

The dehydration reaction of α-glucose has a much larger branching ratio than that of β-glucose, which is consistent with our theoretical prediction. The ratio $r = I(m/z\ 185)/I(m/z\ 143)$, where I represents ion intensity, are 0.72 ± 0.05 and 0.085 ± 0.015, for α-glucose and β-glucose, respectively. We found that these

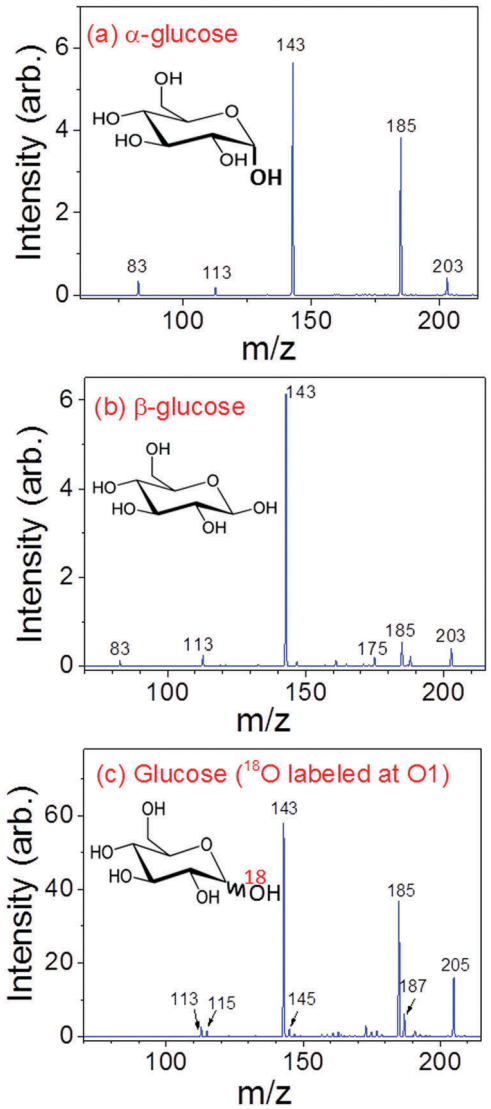

Fig. 8 CID spectra of sodiated (a) α-glucose, (b) β-glucose, and (c) ^{18}O labeled glucose at O1 (mixture of α-glucose and β-glucose) obtained at 40% normalized collision energy.

ratios do not change substantially with the normalized collision energy (20–100%) we used in this study. Thus our results strongly suggest that these ratios can be used to identify the anomeric configuration of glucose. In practical applications, the relationship of ion ratio $I(m/z\ 185)/I(m/z\ 143)$ *vs.* α- and β-glucose ratio in solution has to be established to determine the ratio of these two anomers in a mixture.

Kanie and co-workers measured the loss of sodium cation from sodiated monosaccharide during CID as a function of activation time and collision energy.[49] They found that the activation time for precursor ion intensity to decrease to 50% depends on the collision energy and the anomeric configuration of monosaccharides. Consequently, they suggested that energy resolved mass spectrometry (ERMS) can be used to identify the anomeric configuration of monosaccharides.[49] The identification using ERMS requires the measurement of CID spectra for different activation time and collision energies, which is time consuming. Compared to the ERMS technique, our method provides a simpler and faster identification of anomeric configuration.

The CID spectra of ^{18}O-labeled sodiated glucose (mixture of α-glucose and β-glucose) at the O1 position are shown in Fig. 8(c). The *m/z* 185 and 143 ions represent the elimination of H_2O and $C_2H_4O_2$ which include ^{18}O. They have large intensities, indicating that they are the major dissociation channels and the dissociation barriers must be small. In contrast, the *m/z* 187 and 145 ions represent the elimination of H_2O and $C_2H_4O_2$ which do not contain ^{18}O. They have small intensities, indicating that they are the minor dissociation channels and the dissociation barriers must be high. This is consistent with our theoretical calculations. On the basis of the experimental data and theoretical calculations, we conclude that the dehydration reaction and cross-ring dissociation of sodiated glucose mainly occur at the anomeric carbon of reducing end at low-energy CID.

Acknowledgements

Part of this work was financially supported by the Ministry of Science and Technology, Taiwan (103-2113-M-001-011-MY3).

References

1 R. A. Laine, *Glycobioloby*, 1994, **4**, 759.
2 National Research Council (US) Committee on Assessing the Importance and Impact of Glycomics and Glycosciences: Transforming Glycoscience: A roadmap for the future. National Academies Press, Washington, DC (2012).
3 J. O. Duus, C. H. Gotfredsen and K. Bock, *Chem. Rev.*, 2000, **100**, 4589.
4 E. J. Cocinero, P. Carcabal, T. D. Vaden, J. P. Simons and B. G. Davis, *Nature*, 2011, **469**, 76.
5 E. J. Cocinero, D. P. Gamblin, B. G. Davis and J. P. Simons, *J. Am. Chem. Soc.*, 2009, **131**, 11117.
6 A. Terol, E. Paredes, S. E. Maestre, S. Prats and J. L. Todolí, *J. Sep. Sci.*, 2012, **35**, 929.
7 J. Zaia, *Mass Spectrom. Rev.*, 2004, **23**, 161.
8 H. C. Hsu, M. T. Tsai, Y. A. Dyakov and C. K. Ni, *Int. Rev. Phys. Chem.*, 2012, **31**, 201.
9 F. Munteanand and P. B. Armentrout, *J. Chem. Phys.*, 2001, **115**, 1213.
10 A. L. Heatonand and P. B. Armentrout, *J. Am. Chem. Soc.*, 2008, **130**, 10227.
11 G. E. Hofmeister, Z. Zhou and J. A. Leary, *J. Am. Chem. Soc.*, 1991, **113**, 5964.
12 M. R. Asam and G. L. Glish, *J. Am. Soc. Mass Spectrom.*, 1997, **8**, 987.
13 E. V. da Costa, A. S. P. Moreira, F. M. Nunes, M. A. Coimbra, D. V. Evtuguin and M. R. M. Domingues, *Rapid Commun. Mass Spectrom.*, 2012, **26**, 2897.
14 H. Zhang, S. M. Brokman, N. Fang, N. L. Pohl and E. S. Yeung, *Rapid Commun. Mass Spectrom.*, 2008, **22**, 1579.

15 A. Carroll, D. Willard and C. B. Lebrilla, *Anal. Chim. Acta*, 1995, **307**, 431.
16 B. Mulroney, J. C. Traeger and B. A. Stone, *J. Mass Spectrom.*, 1995, **30**, 1277.
17 D. J. Harvey, *J. Am. Soc. Mass Spectrom.*, 2005, **16**, 622.
18 D. Ashline, S. Singh, A. Hanneman and V. Reinhold, *Anal. Chem.*, 2005, **77**, 6250.
19 W. Jiang, V. H. Wysocki, E. D. Dodds, R. I. Miesfeld and P. Y. Scaraffia, *Anal. Biochem.*, 2010, **404**, 40.
20 S. Lee, S. J. Valentine, J. P. Reilly and D. E. Clemmer, *Int. J. Mass Spectrom.*, 2012, **309**, 161.
21 G. I. Csonka, A. D. French, G. P. Johnson and C. A. Stortz, *J. Chem. Theory Comput.*, 2009, **5**, 679.
22 M. Appell, G. Strati, J. L. Willett and F. A. Momany, *Carbohydr. Res.*, 2004, **339**, 537.
23 F. A. Momany, M. Appell, G. Strati and J. L. Willett, *Carbohydr. Res.*, 2004, **339**, 553.
24 M. Appell, J. L. Willett and F. A. Momany, *Carbohydr. Res.*, 2005, **340**, 459.
25 F. A. Momany, M. Appell, J. L. Willett and W. B. Bosma, *Carbohydr. Res.*, 2005, **340**, 1638.
26 F. A. Momany, M. Appell, J. L. Willett, U. Schnupf and W. B. Bosma, *Carbohydr. Res.*, 2006, **341**, 525.
27 B. Y. Ma, H. F. Schaefer and N. L. Allinger, *J. Am. Chem. Soc.*, 1998, **120**, 3411.
28 C. J. Cramer and D. G. Truhlar, *J. Am. Chem. Soc.*, 1993, **115**, 5745.
29 A. L. Heaton and P. B. Armentrout, *J. Phys. Chem. A*, 2008, **112**, 10156.
30 H. Wincel, *J. Am. Soc. Mass Spectrom.*, 2011, **22**, 1570.
31 M. Alcami, A. Luna, O. Mo, M. Yanez, L. Boutreau and J. Tortajada, *J. Phys. Chem. A*, 2002, **106**, 2641.
32 R. S. Assary, P. C. Redfern, J. R. Hammond, J. Greeley and L. A. Curtiss, *J. Phys. Chem. B*, 2010, **114**, 9002.
33 M. R. Nimlos, X. Qian, M. Davis, M. E. Himmel and D. K. Johnson, *J. Phys. Chem. A*, 2006, **110**, 11824.
34 R. S. Assary, P. C. Redfern, J. Greeley and L. A. Curtiss, *J. Phys. Chem. B*, 2011, **115**, 4341.
35 H. Suzuki, A. Kameyama, K. Tachibana, H. Narimatsu and K. Fukui, *Anal. Chem.*, 2009, **81**, 1108.
36 J. L. Chen, C. Lee, I. C. Lu, C. L. Chien, Y. T. Lee, W. P. Hu and C. K. Ni, *J. Mass Spectrom.*, 2016, **51**, 1180.
37 B. J. Bythell, M. T. Abutokaikah, A. R. Wagoner, S. Guan and J. M. Rabus, *J. Am. Soc. Mass Spectrom.*, 2017, **28**, 6883.
38 Y. Tan and N. C. Polfer, *J. Am. Soc. Mass Spectrom.*, 2015, **26**, 359.
39 C. Konda, B. Bendiak and Y. Xia, *J. Am. Soc. Mass Spectrom.*, 2012, **23**, 347.
40 P. J. Stephens, F. J. Devlin, C. F. Chabalowski and M. J. Frisch, *J. Phys. Chem.*, 1994, **98**, 11623.
41 M. Marianski, A. Supady, T. Ingram, M. Schneider and C. Baldauf, *J. Chem. Theory Comput.*, 2016, **12**, 6157.
42 Y. Zhao, B. J. Lynch and D. G. Truhlar, *Phys. Chem. Chem. Phys.*, 2005, **7**, 43.
43 M. J. Frisch, G. W. Trucks, H. B. Schlegel, G. E. Scuseria, M. A. Robb, J. R. Cheeseman, G. Scalmani, V. Barone, B. Mennucci, G. A. Petersson, H. Nakatsuji, M. Caricato, X. Li, H. P. Hratchian, A. F. Izmaylov, J. Bloino, G. Zheng, J. L. Sonnenberg, M. Hada, M. Ehara, K. Toyota, R. Fukuda, J. Hasegawa, M. Ishida, T. Nakajima, Y. Honda, O. Kitao, H. Nakai, T. Vreven, J. A. Montgomery, Jr., J. E. Peralta, F. Ogliaro, M. Bearpark, J. J. Heyd, E. Brothers, K. N. Kudin, V. N. Staroverov, R. Kobayashi, J. Normand, K. Raghavachari, A. Rendell, J. C. Burant, S. S. Iyengar, J. Tomasi, M. Cossi, N. Rega, J. M. Millam, M. Klene, J. E. Knox, J. B. Cross, V. Bakken, C. Adamo, J. Jaramillo, R. Gomperts, R. E. Stratmann, O. Yazyev, A. J. Austin, R. Cammi, C. Pomelli, J. W. Ochterski, R. L. Martin, K. Morokuma, V. G. Zakrzewski, G. A. Voth, P. Salvador, J. J. Dannenberg, S. Dapprich, A. D. Daniels, Ö. Farkas, J. B. Foresman, J. V. Ortiz, J. Cioslowski and D. J. Fox, *Gaussian 09, Revision E.01*, Gaussian, Inc., Wallingford CT, 2009.
44 H. Satoh, T. Oda, K. Nakakoji, T. Uno, H. Tanaka and K. Ohno, *J. Chem. Theory Comput.*, 2016, **12**, 5293.
45 H. B. Mayes, L. J. Broadbelt and G. T. Beckham, *J. Am. Chem. Soc.*, 2014, **136**, 1008.
46 T. Yamagaki, K. Fukui and K. Tachibana, *Anal. Chem.*, 2006, **78**, 1015.
47 Y. Nishimura, D. Yokogawa and S. Irle, *Chem. Phys. Lett.*, 2014, **603**, 7.
48 W. Pigman and H. S. Isbell, *Adv. Carbohydr. Chem.*, 1968, **23**, 11.
49 Y. Shioiri, K. Suzuki, S. Daikoku, A. Kurimoto, Y. Ito and O. Kanie, *Carbohydr. Res.*, 2013, **382**, 43–51.

